

Research Article

Enhancements of G3-PLC Technology for Smart-Home/Building Applications

Luca Di Bert, Salvatore D'Alessandro, and Andrea M. Tonello

Dipartimento di Ingegneria Elettrica, Gestionale e Meccanica (DIEGM), Università di Udine, 33100 Udine, Italy

Correspondence should be addressed to Andrea M. Tonello; tonello@uniud.it

Received 30 September 2012; Accepted 19 December 2012

Academic Editor: Ahmed Zeddami

Copyright © 2013 Luca Di Bert et al. This is an open access article distributed under the Creative Commons Attribution License, which permits unrestricted use, distribution, and reproduction in any medium, provided the original work is properly cited.

To enable the smart grid concept, it is fundamental to consider the in-home/building context where, beside the conventional home networking services, home automation and smart energy management services have to be offered. In this paper, we consider the in-home/building scenario, for which we propose a convergent network architecture to enhance the performance of the narrowband power line communication (PLC) G3-PLC technology through its integration with an Ethernet-based network. To this end, we define the protocols characterizing the network modules, namely, switches and routers, which allow for integrating the G3-PLC with Ethernet devices. Since Ethernet represents a convergent standard for many communication devices, by adding this functionality to G3-PLC, interconnectivity with other heterogeneous nodes can be offered. Furthermore, since the G3-PLC medium access control layer is based on a carrier sense multiple access scheme, its performance decreases when the number of network nodes contending for the channel increases. Therefore, we evaluate the network performance when an optimized time division multiple access scheme is adopted. The proposed convergent network architecture has been implemented in the OMNeT++ network simulator.

1. Introduction

Energy efficiency and power saving were identified in 2010 as fundamental objectives to contribute to the sustainable growth specified in the “Europe 2020” strategy [1]. As a consequence, in the near future, the power grid needs to become a distributed large-scale system that has to smartly manage flows of electricity produced by big or small plants, that is, a smart grid (SG). To this respect, demand side and demand response mechanisms have to be implemented, so that prosumers will actively collaborate in the use and delivery of energy [2, 3]. To enable the SG concept, it becomes therefore fundamental to consider the in-home/building context where, beside the conventional home networking services—for example, triple play (high speed internet access, television, telephone), infotainment, and resource sharing in local area networks (LANs)—, home automation and smart energy management services have to be offered.

Differently from home networking services, home automation and energy management services usually involve a large number of nodes (sensors/actuators) that are pervasively deployed within the house/building and transmit

a small amount of data. Despite the small amount of data, strict requirements as coverage, latency, delay, and robustness must be fulfilled for some applications, for example, the automation of windows and doors, the control of heating, ventilation and air conditioning (HVAC), the monitoring of presence/temperature/gas/smoke, the management of loads, and so forth.

In this context, power line communication (PLC) is a key technology since (a) the power line grid is pervasively deployed within houses/buildings, and (b) it does not require the use of new wires, which, in turn, reduces deployment costs.

PLC devices are in general grouped into two categories, that is, narrowband (NB) and broadband (BB) devices, according to the bit-rate that they can offer. BB-PLC devices are widely deployed to offer high speed home networking services. They work in the frequency band 2–30 MHz (and beyond) and make use of advanced modulation techniques to offer bit-rates in the order of hundreds of Mbps. On the other hand, NB-PLC devices have been developed to offer low bit-rates for home automation (indoor) and smart metering (outdoor) services. These devices usually work in a frequency

band belonging to the range of 3–490 kHz, depending on the regulations applied in a specific country, for example, CENELEC, ARIB, FCC. Detailed information regarding BB and NB PLC technologies can be found in [4].

Clearly, besides PLC, there is also a broad variety of wireless and wired technologies that can be used for both high and low bit-rate in-home applications [5], for example, WiFi, Zigbee, Bluetooth, Z-Wave, twisted pair Ethernet, MoCA, and so forth.

Despite the existence in the market of this broad variety of communication technologies, the bottleneck to their pervasive deployment, and thus to the joint delivery of different services, is that they often cannot interconnect and interoperate, and in some cases even coexist.

1.1. Smart Home/Building Enabled by a Convergent Network.

From the previous discussion, we deem important to realize a convergent communication network in order to integrate a broad variety of communication technologies thus to enable the smart home (SH) concept, that is, the joint delivery of home networking, home automation and energy management services.

The convergent communication network can be obtained by providing a convergent layer where heterogeneous communication technologies can coexist and be interconnected.

Usually, the coexistence, that is, the ability of sharing the same physical medium by two or more devices, is obtained by exploiting different frequency bands at the physical (PHY) layer, or through the use of medium access control (MAC) protocols. The interconnectivity—namely, the capability of devices to exchange data at PHY, data link layer (DLL), and network layer—requires coexistence, and it can be achieved with a convergent layer above the data link layer or at the network layer. Coexistence and connectivity among different technologies, through PHY or data link layer (DLL) mechanisms, have been the focus of many studies. Representative examples are as follows: the inter-PHY protocol developed within the IEEE P1901 working group that allows coexistence among two different broadband PLC devices [6]; the ITU-T G.hn standard that has been conceived with the aim of offering interconnectivity among in-home high speed communication devices working over telephone wires, power lines, and coax [6, 7] (G.hn specifies the PHY layer and the MAC sublayer and addresses the coexistence between protocols that operate on different media); the solution developed within the EU-FP7 OMEGA project, according to which devices belonging to the OMEGA network share the same inter-MAC sublayer and consequently they can coexist and they can be interconnected [8].

Connectivity among heterogeneous devices can be also reached at network layer by exploiting the Internet protocol (IP). The use of the TCP/IP protocol stack to integrate different communication technologies for SH and SG applications is largely advocated. Previous work that follows this approach is described in [3, 9–12] and references therein. Also standardization working groups are considering it, for example, at the end of 2010, IEEE launched the P1905 working group [13] that is focused on the definition of an abstraction layer for multiple home networking technologies. The abstraction

layer will provide a common data and control Service Access Point (SAP) for the home networking technologies described in the IEEE P1901, 802.11 [14], 802.3 [15], and MoCA 1.1 specifications [16]. Finally, a number of standard development groups—among which ZigBee [17], HomePlug [18], and Wi-Fi alliances—are working on the development of the ZigBee Smart Energy version 2.0 [19] that will offer IP-based control for advanced metering infrastructures and home area networks allowing for interoperability with 802.11 and HomePlug devices.

1.2. Contribution. In this paper, we consider the in-home scenario where we propose the use of a convergent network to enhance the performance of NB G3-PLC technology [20, 21] through its integration in an Ethernet network. We thus focus on the convergence at the DLL. Clearly, the integration of the proposed network in a TCP/IP network can be easily obtained by adding the corresponding transport/network layers. It should be noted that G3-PLC was mostly designed for outdoor SG applications. Furthermore, it has been used as a baseline technology for the development of the [22] IEEE P1901.2 and the ITU-T G.hnem standard for SG applications. The deployment of G3-PLC in home/buildings is indeed interesting. However, in our previous work [23], we have found, through experimental test campaigns, that the G3-PLC technology can exhibit poor performance within large houses/buildings. Therefore, in this paper, we propose possible enhancements focusing at the MAC DDL sublayer.

The first contribution of this paper is the definition of the protocols characterizing the network modules, namely, switches and routers, which allow the integration of G3-PLC and Ethernet devices in a convergent network architecture. Range extension is achieved by partitioning the overall network into subnetworks, that is, G3-PLC subnetworks. An Ethernet backbone (in particular using cat5 wiring) provides connectivity between the subnetworks.

The second contribution regards the evaluation of the convergent network when adopting a time division multiple access (TDMA) scheme at the MAC sublayer of the G3-PLC nodes. In fact, the G3-PLC MAC sublayer is based on the non-beacon-enabled mode of the IEEE 802.15.4 standard, which is a carrier sense multiple access (CSMA) scheme. As it is known, the performance of CSMA schemes decreases as the number of the network nodes contending for the channel increases. This situation can occur in large houses/buildings where a large number of sensors/actuators is deployed. To cope with this problem, we implement a modified version of the beacon-enabled mode of the IEEE 802.15.4 [24], which is based on a TDMA MAC mechanism, and we show that substantial performance increase can be obtained.

The network performance has been evaluated with the use of the OMNeT++ network simulator [25].

The remainder of the paper is as follows. In Section 2, we briefly describe the G3-PLC and the Ethernet technologies. Then, in Section 3, we present the implementation of the convergent network, and in Section 4, we study its performance. Finally, in Section 5, we consider the TDMA implementation and we compare its performance with CSMA. Conclusions follow in Section 6.

2. Communication Technologies

In this section, we describe the G3-PLC and the Ethernet technologies that will be used to build the convergent in-home network in Section 3.

2.1. G3-PLC. Originally developed for Automatic Metering Management (AMM) applications, G3-PLC is playing a relevant role inasmuch it has been used for the development of the IEEE P1901.2 and the ITU-T G.hnem standard for SG applications [22]. In the following, we discuss its PHY layer and MAC sublayer.

2.1.1. PHY Layer. According to [20], the G3-PLC technology has been designed to support CENELEC, ARIB, and FCC bands in the frequencies range between 10 kHz and 490 kHz. It makes use of pulse shaped—orthogonal frequency division multiplexing (PS-OFDM) carrying DQPSK, or DBPSK symbols in “normal” or “robust” mode. The correspondent maximum data packet is 235 bytes with DQPSK, 235 bytes with DBPSK in “normal” mode, and 133 bytes with DBPSK in “robust” mode. The maximum achievable bit-rate is 33.4 kbps using DQPSK. It should be noted that the differential encoding takes place across the data stream of each subchannel.

The PHY frame format (see Figure 1) is characterized by (i) the preamble, which is a multisymbol field used to perform carrier sense operations, to enable control functions and to synchronize the receiver and the transmitter, (ii) the frame control header (FCH), which carries control information required to correctly demodulate the received signal, (iii) the data payload. The data payload length (n) depends on the transmission mode, that is, normal and robust. In normal mode, the forward error correction (FEC) is performed through a Reed Solomon (RS) encoder and a convolutional encoder, whereas the error check is done with a frame check sequence (FCS). In robust mode, beside RS and convolutional encoding, there is a repetition code (RC) that repeats each bit following the preamble 4 times. At the receiver side, the hard decision Viterbi decoder and the RS decoder are used.

When showing simulation results, we consider G3-PLC working in the CENELEC-A band (despite the fact that CENELEC-A is generally not used for home networking, performance is not significantly affected by the operating band). In this case, it uses PS-OFDM with a raised cosine window, and $M = 256$ subchannels out of which $N_c = 36$ are used in the 35.9–90.6 kHz frequency band. Furthermore, we assume the PHY frame to last $N_s = 40$ OFDM symbols that carry data modulated with DQPSK and robust DBPSK. This assumption, respectively, leads to $n = 163$ or $n = 13$ bytes of data and 16 or 8 RS parity check bytes. Consequently, the maximum achievable bit-rates are 29.6 kbps and 2.4 kbps. Table 1 reports the set of the PHY layer parameters.

2.1.2. MAC Sublayer. According to [21], the MAC sublayer is based on the IEEE 802.15.4-2006 specification for low-rate wireless personal area networks (WPANs) [24]. Basically, the channel access method is based on the CSMA with collision avoidance (CSMA/CA) mechanism and a random

TABLE 1: G3-PLC system specifications.

Number of PS-OFDM symbols	$N_s = 40$
Number of IFFT/FFT points	$M = 256$
Number of used subchannels	$N_c = 36$
Number of overlapped samples	$N_o = 8$
Number of cyclic prefix samples	$N_{CP} = 30$
Number of FCH symbols	$N_{FCH} = 13$
Sampling frequency (MHz)	$f_s = 0.4$
Number of preamble symbols (without FCH)	$N_{pre} = 9.5$

Preamble	FCH	Data n bytes	RS parity	FCS 2 byte
----------	-----	-----------------	-----------	---------------

FIGURE 1: G3-PLC PHY frame format.

backoff time. It is worth noting that G3-PLC does not provide specifications for the higher ISO/OSI layers.

The MAC implementation starts from the assumption of a minimum overhead of 8 bytes. Therefore, according to the amount of data bytes defined in the PHY, the maximum MAC payload is 155 bytes in normal mode and 5 bytes in robust mode. For the sake of implementation simplicity, we assume that the transmission does not wait for any current reception acknowledgement (ACK).

2.2. Ethernet. Ethernet is widely deployed on LANs. It offers a convergent logical link control (LLC) sublayer for many different PHY layers and MAC sublayers, for example, coax, twisted pair as well as optical fiber and wireless. Although the Ethernet protocol was originally proposed for use over coax cables, most of today’s Ethernet networks make use of twisted pairs and operate in full duplex mode: the network is switched thus the connections are handled point-to-point and cannot be shared by multiple devices. Therefore, the full duplex mode eliminates carrier sense multiple access with collision detection (CSMA/CD) mechanisms because there is no need to determine whether the connection is already being used.

In this perspective, we decided to consider the 100BASE-TX, that is, the predominant form of Fast Ethernet (IEEE 802.3u) over twisted pair cables (cat5), offering bit-rates up to 100 Mbps. Moreover, since 100BASE-TX is full-duplex, it requires the use of switches.

3. Convergent Network Implementation

In this paper, we focus on the integration of G3-PLC technology within an Ethernet network. Since the switched Ethernet network exhibits a star topology and the power line channel can be considered as a bus, we adopt a treelike topology—as a combination of bus and star topologies—to implement the convergent network (see Figure 2). The major benefit deriving from the use of such a topology is its ability to be scalable, extensible, and reliable. The convergence between Ethernet and G3-PLC can be obtained through the definition of a shared common layer that provides interconnectivity among heterogeneous lower layers.

The network convergence is achieved by defining different network devices, that is, *end nodes*, *routers*, and *switches*.

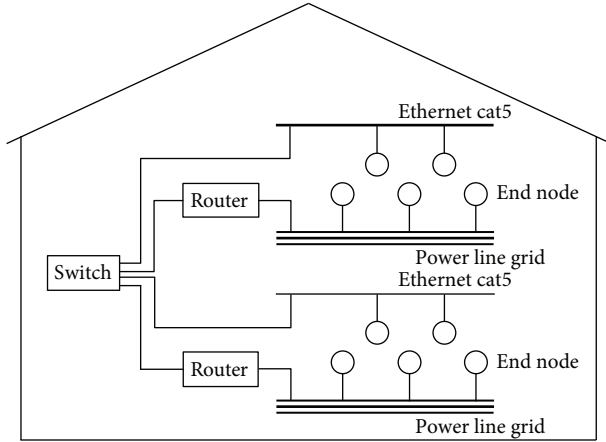


FIGURE 2: Network topology.

3.1. End Nodes. They represent the devices of the network that directly interact with the surrounding environment, for example, sensors, actuators, switches, meters, and so on. These nodes are grouped into subnetworks according to the same communication technology, that is, G3-PLC. From a logical point of view, the end nodes can be all characterized by the same building blocks, that is, a traffic generator (which is responsible of data packets generation) and the network adapter. The network adapter comprises a PHY, a MAC, and a buffer of data packets coming from the traffic generator.

3.2. Router. Since G3-PLC does not provide any specification for the integration in a switched Ethernet network, we need a network device that groups G3-PLC nodes into a subnetwork and integrates the subnetwork with the rest of the Ethernet network. To do that, we define a router that offers network adapters towards both Ethernet and G3-PLC. Beside the network adapters, the Router has a routing module that is responsible of translating and forwarding packets from one network adapter to the other and vice versa: this module is responsible of interconnectivity between Ethernet and G3-PLC. It is worth noting that since the maximum allowed G3-PLC PHY frame size is 251 bytes (corresponding to a payload of 235 data bytes both in DQPSK and DBPSK normal mode), the router encapsulates each G3-PLC frame into one Ethernet frame, whose maximum payload dimension is 1500 bytes. On the other side, Ethernet frames exceeding 251 bytes are fragmented by the router in order to fulfill G3-PLC constraints. However, this assumption is not necessarily optimal.

As depicted in Figure 3, the routing module keeps trace of packets received from its subnetwork nodes, and it generates a forwarding table with *source address*, *insertion time*, and *link quality*. In this perspective, the router dynamically learns about the existence of nodes during reception of packets and modifies its table updating the link quality or removing aged entries, according to the insertion time. It is worth noting that a given subnetwork can be managed by two (or more) routers in order to ensure a more reliable communication on harsh power line channels, or equally, to increase the network coverage. Furthermore, in order to prevent loops, the router

is able to recognize and discard packets directly arrived from other routers.

3.3. Switch. The switch is a well-known network device. As depicted in Figure 4, the switch has been modified in order to work seamlessly with the routers. In particular, it is able to build and update a forwarding table exploiting nodes information harvested by each router. A forwarding table entry is composed of *source address*, *insertion time*, *link quality*, and *arrival port number*. Therefore, the switch compares the information carried by a packet with the correspondent table entries and forwards the packet to the correct port (or broadcast if the destination address has no correspondence in the table). In this case, the insertion time parameter is exploited to remove aged entries from the table and thus increasing the system fault tolerance. Again, the switch is able to prevent packet loops. We also point out that since link quality is updated periodically, the switch is able to dynamically handle the network changes. It is now clear that the combination of the router and switch procedures enables the integration of heterogeneous communication technologies leading to a convergent network. Moreover, this combination provides the basis for satisfying quality of service (QoS) constraints.

It should be finally noted that the integration of G3-PLC with Ethernet easily allows for integrating the G3-PLC technology in IP networks.

4. Simulation Setup and Results

The convergent network has been implemented using the OMNet++ simulator and its extension INET-Framework [26]. OMNet++ is an open source, component-based simulation library, and framework that is primarily thought for building network simulators. Basic components, that is, *simple modules*, are programmed in C++ and then combined into larger components, that is, *compound modules*, using a network description (NED) language. NED language is also used to connect compound modules and assemble the whole network. A screenshot of the simulated network is shown in Figure 5 where we assume a cat5 cable propagation delay of 500 ns.

In order to quantify the convergent network performance, we define a representative metric, namely, the aggregate network throughput (THR). It is evaluated as

$$\text{THR} = \sum_{u=1}^N \text{THR}^{(u)} \text{ [bps]}, \quad (1)$$

where N is the number of network nodes and $\text{THR}^{(u)}$ is the average throughput achieved by the u th node, which is obtained as

$$\text{THR}^{(u)} = 8nN_g^{(u)} \text{ [bps]}, \quad (2)$$

where n are the data bytes encapsulated in the PHY frame, $N_g^{(u)}$ is the number of correct received PHY frames per second by the u th node, which are detected exploiting either

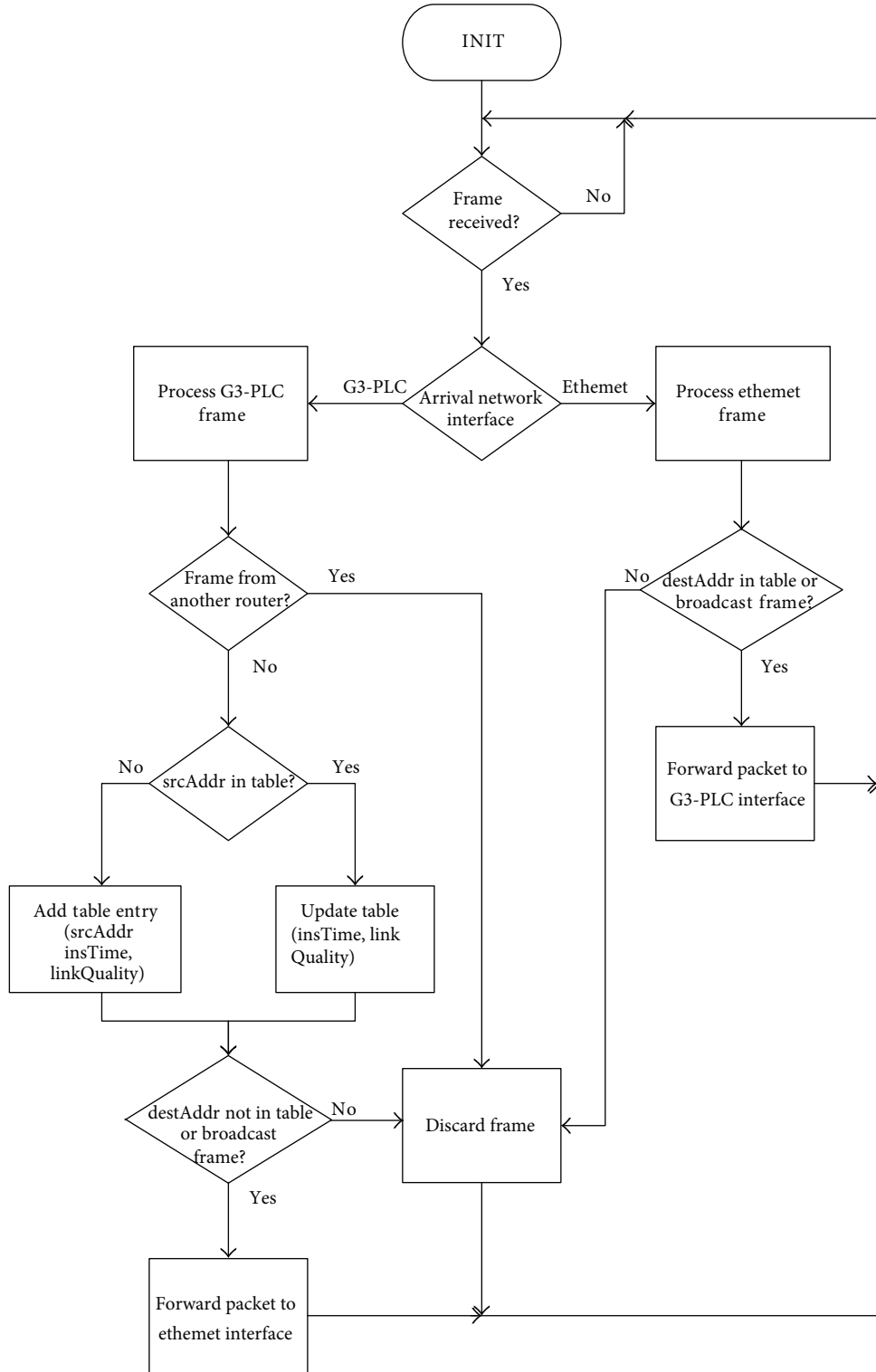


FIGURE 3: Router flow chart.

the knowledge of the transmitted frame or the FCS field. Furthermore, we define the frame error rate (FER) as follows:

$$FER^{(u)} = \frac{(N_t^{(u)} - N_g^{(u)})}{N_t^{(u)}}, \quad (3)$$

where $N_t^{(u)}$ is the total number of transmitted frames destined to u th user. It is worth noting that the FER takes into account corrupted frames as well as missed frames.

In order to model the power line channel in the OMNeT++ implementation, we make use of the hardware

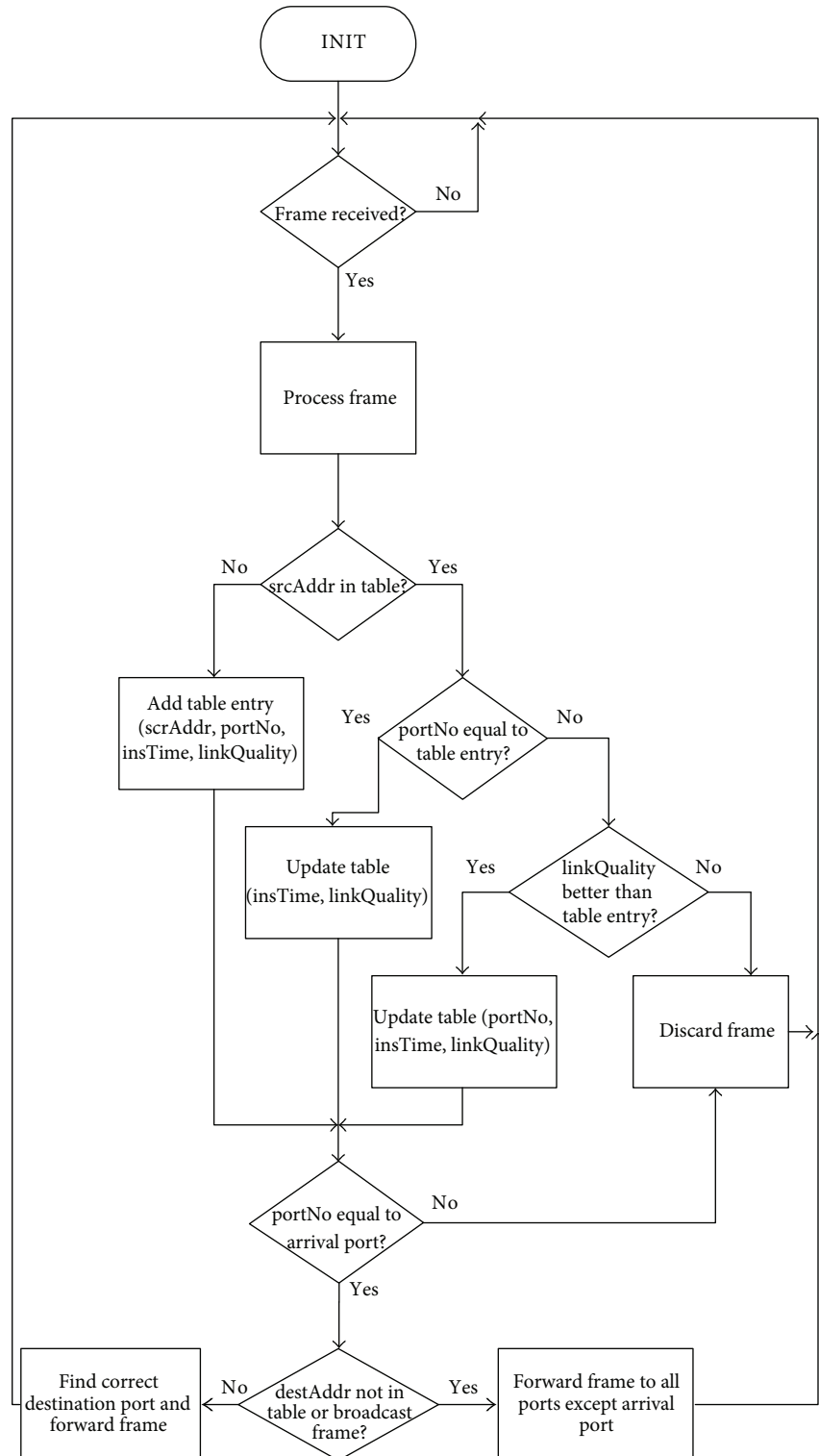


FIGURE 4: Switch flow chart.

platform [27] that consists of a pair of NB-PLC OFDM based modems whose parameters are very similar to the ones specified by G3-PLC (see Section 2). We have performed two trial campaigns connecting, at each time, this pair of modems to two power sockets within a house. The first campaign took place in a single floor house. Whereas, the second took place

in a three-floor house, whose electrical power is distributed from the main panel (MP) to each floor through a floor circuit breaker (CB) located at the MP. In the latter case, we have considered either the transmission between outlets belonging to the same floor or between outlets belonging to different floors. Appliances, for example, television, washing machine,

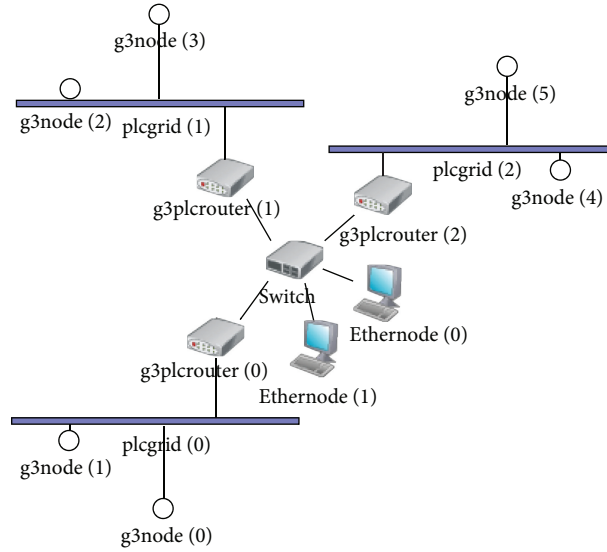


FIGURE 5: Screenshot of an example of convergent network simulation in OMNET++.

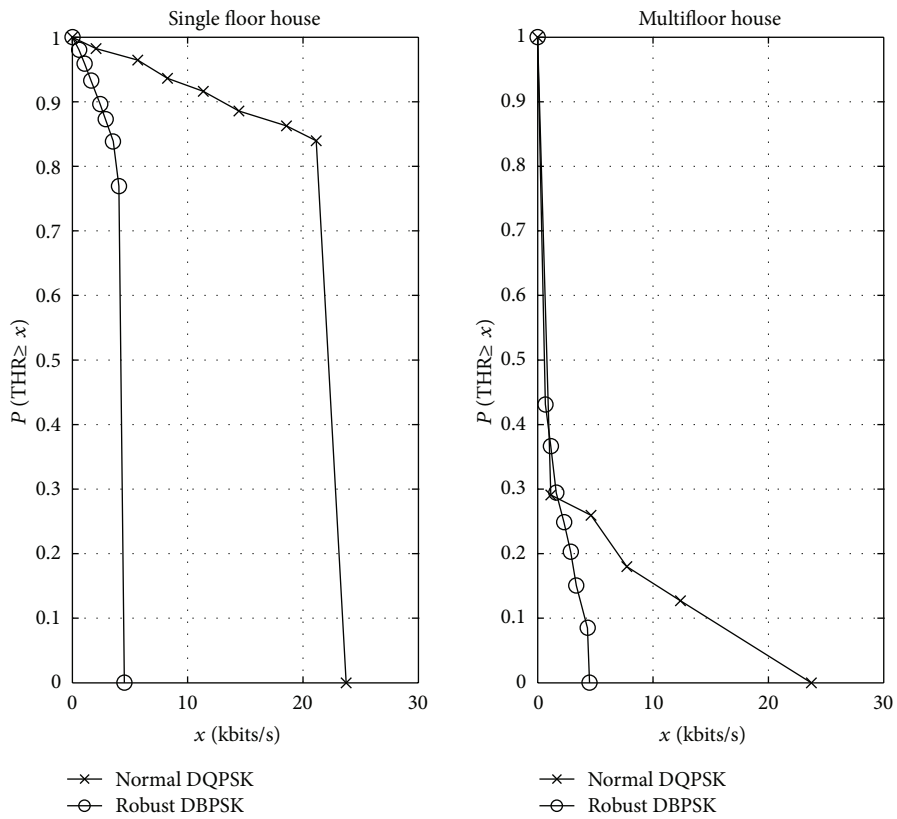


FIGURE 6: CCDF of the measured THR for G3-PLC technology.

battery charger, fluorescent lamps, fridge, and so on, have been plugged and unplugged.

Figures 6 and 7, respectively, show the complementary cumulative distribution function (CCDF) of the THR, and the cumulative distribution function (CDF) of the FER for normal and robust mode for both the considered scenarios. As we can see, both the THR and the FER are much more

degraded for channels belonging to the multifloor house. This is simply explainable observing that channels associated to multifloor houses cover in average larger distances than those in single floor houses, and they experience higher attenuation. From the obtained results, we computed the distribution of the FER. In particular, for the single floor house, the FER can be assumed to be exponentially distributed with mean

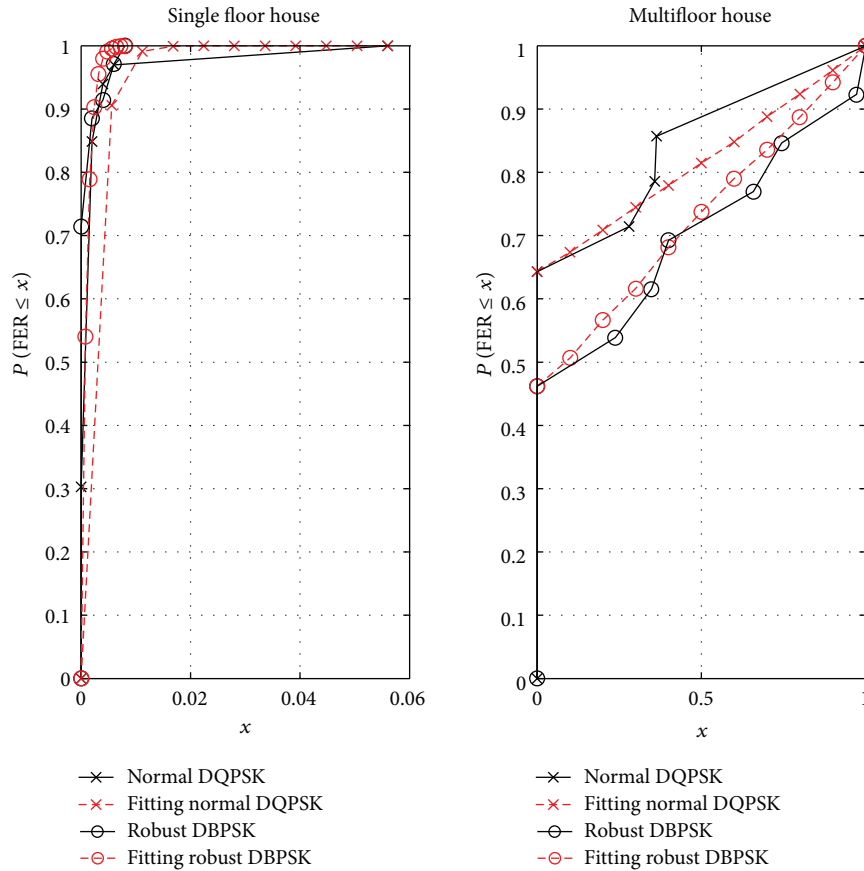


FIGURE 7: CDF of the measured FER for G3-PLC technology. The distribution fitting is also shown.

equal to 0.0024 and 0.001, respectively, for normal DQPSK and robust DBPSK mode. Regarding the multifloor house, we model the FER as uniformly distributed in the range (0.6429, 1) or (0.4615, 1), respectively, for normal DQPSK and robust DBPSK mode. The obtained statistics are depicted in Figure 7 (red dotted lines). More results regarding the test campaigns are reported in [23].

It is important to note that in the case of a multi-floor house, the G3-PLC network can be naturally split into several subnetworks, one for each floor. The subnetworks can then be connected through Ethernet. The same architecture can be used in large buildings that may already have a wired Ethernet deployment.

We now turn our attention to the convergent network behavior. To do that, we consider the saturation throughput (STH), which is defined as the limit reached by the THR when the offered load increases, and it represents the maximum load that the system can carry [28]. In STH conditions, each node has immediately a packet available for transmission, after the completion of each successful transmission.

Now we build the simulation scenario using from 6 up to 60 G3-PLC nodes and we evaluate the STH when no Routers are introduced, and when two and three Routers—for example, one per each floor—are considered. The traffic is generated among G3-PLC nodes belonging to the same subnetwork or to different subnetworks in DQPSK mode.

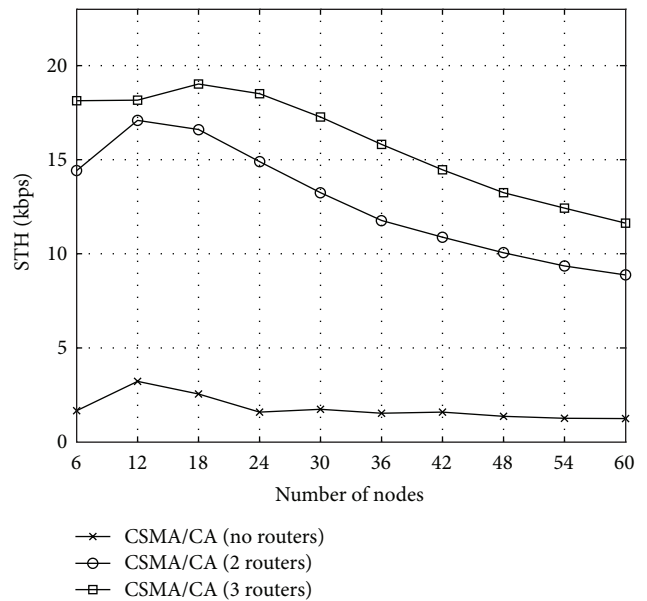


FIGURE 8: Simulated STH for different network configurations.

Figure 8 shows the STH. As we can see, the introduction of 2 and 3 routers substantially improves the performance. It is worth noting that the STH improvements directly translate in a coverage increase.

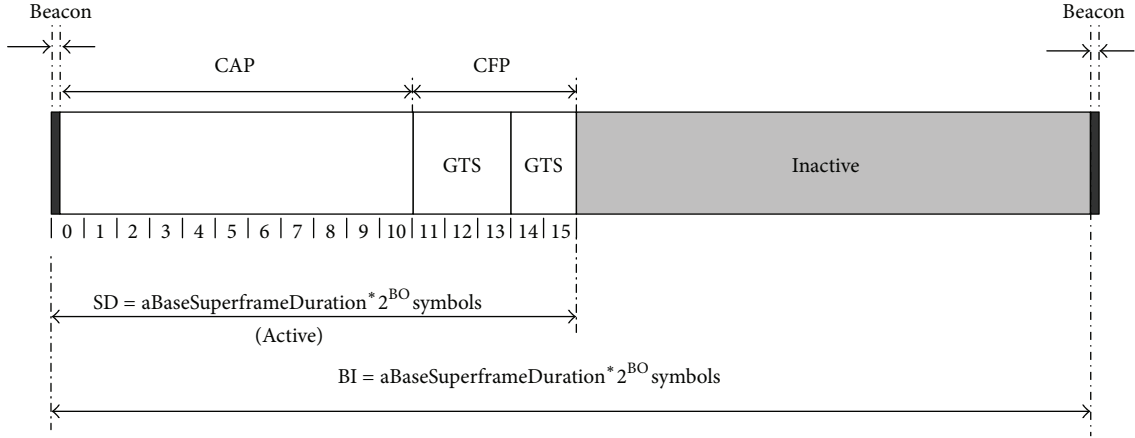


FIGURE 9: An example of superframe structure [24].

TABLE 2: Superframe parameters and values.

Parameters	Value
$aBaseSuperframeDuration$	$aBaseSlotDuration * aNumSuperframeSlots$
$aBaseSlotDuration$	50
$aNumSuperframeSlots$	16
SO = BO	2

5. Further Improvements Using Time Division Multiple Access

Despite the STH improvements related to the introduction of routers, the bottleneck of the network is represented by the degradation of the performance with the increasing number of G3-PLC nodes within each subnetwork (see Figure 8). To prevent this occurrence, we envision the G3-PLC communication technology proposing a different channel access method that provides a higher QoS, namely, time division multiple access (TDMA). To do this, we implement the *beacon-enabled* mode of the IEEE 802.15.4-2006 specifications [24]. It defines a *superframe* structure as depicted in Figure 9. Each superframe is characterized by an active and an inactive portion. The active portion, which is defined by the superframe duration (SD), consists of a contention access period (CAP) and a contention-free period (CFP). In the CAP period, data packet transmission follows a CSMA/CA algorithm while during the CFP the channel access is based on TDMA. The network coordinator, represented by the router, assigns a guaranteed time slot (GTS) to each node. We notice that the coordinator may assign more than one GTS to each station, in order to satisfy given QoS constraints. Therefore, the CFP grows or shrinks dynamically fulfilling the minimum CAP length (440 symbols). We further denote with N_{TStot} the number of time slots present in the CFP.

It is worth noting that the beacon frame, which is periodically sent by the WPAN coordinator for synchronization purposes, can be replaced by synchronization via the exploitation of the mains cycle.

The values of the parameters used in beacon-enabled mode simulations are reported in Table 2.

The GTS assignment is done by each router solving the following optimization problem:

$$\begin{aligned} \max_{\underline{N}_{TS}} \quad & \sum_{u=1}^N \frac{N_{TS}^{(u)}}{N_{TStot}} \text{THR}^{(u)} \\ \text{s.t.} \quad & \sum_{u=1}^N \frac{N_{TS}^{(u)}}{N_{TStot}} = 1, \end{aligned} \quad (4)$$

$$\frac{N_{TS}^{(u)}}{N_{TStot}} \text{THR}^{(u)} \geq p^{(u)} \text{THR}^{(u)}, \quad \forall u = 1, \dots, N,$$

where N is the number of nodes, $N_{TS}^{(u)}$ is the number of time slots assigned to node u , and $\underline{N}_{TS} = [N_{TS}^{(1)}, N_{TS}^{(2)}, \dots, N_{TS}^{(N)}]$. Furthermore, $\text{THR}^{(u)}$ is the throughput of node u in bps. It can be obtained as $\text{THR}^{(u)} = 8n(1 - \text{FER}^{(u)})/T_s$, with T_s denoting the time slot duration in seconds. $p^{(u)} \in [0, 1]$ are QoS coefficients, each indicates the percentage of the throughput that the u th node has to achieve with respect to the one that it would achieve in the corresponding single user scenario. Finally, the condition in the second line of (4) forces all the time slots in a CFP to be used.

Problem (4) is an integer linear programming problem. Therefore, it is, in general, NP hard. To simplify the problem, we solve (4) using linear programming (LP) and we round the obtained coefficients to the lower closest integer value. Clearly, there could be cases where the number of slots assigned to one or more nodes is zero. In these cases, the correspondent nodes are deferred to transmit in the CAP. Furthermore, when some time slots are not occupied as result of the rounding of the coefficients, these will be assigned to the nodes that have the highest throughput, leaving the CAP free of transmissions. Finally, we assume $\sum_{u=1}^N p^{(u)} \leq 1$. The latter assures that the LP always give a feasible solution if $N \leq N_{TStot}$.

It is easy to prove that when $\sum_{u=1}^N p^{(u)} = 1$, for example, $p^{(u)} = 1/N$, the optimal solution to (4) can be found

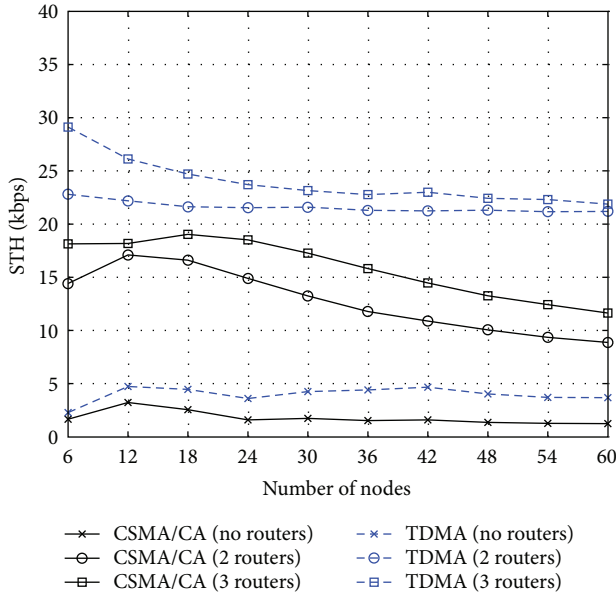


FIGURE 10: STH comparison between CSMA/CA and TDMA.

imposing the Karush Kuhn Tucker (KKT) conditions [29] and it is given by $N_{TS}^{(u)} = N_{TStot}/N$ for all $u = 1, \dots, N$. In the following, we assume the last condition holds true.

Now, in Figure 10, we consider the comparison between the CSMA/CA and the optimized TDMA increasing the number of network nodes. From Figure 10, we notice that the TDMA scheme allows for a substantial increase of the aggregate network throughput with respect to CSMA. Furthermore, it solves the bottleneck problem of CSMA represented by a considerable degradation of the performance with the increasing number of nodes within each subnetwork. We finally notice that the minimum CAP length constraint, specified by the 802.15.4 standard, affects the behavior of the aggregate throughput. In fact, the throughput exhibits a faster decay when considering 2 and 3 routers with respect to the no router case. This is because the negative effect of the CAP is present in each subnetwork, namely twice or three times, respectively.

6. Conclusions

G3-PLC devices show poor performance when working over large in-home/building PLC networks whose links can be severely attenuated. A convergent network, consisting of Ethernet and G3-PLC devices, can be built using routers and switches nodes to cope with this problem. Through simulation results, obtained implementing the convergent network in the OMNET++ simulator, we have shown the feasibility of such a solution. After that, we have analysed the behavior of the CSMA/CA protocol implemented in the G3-PLC devices and we have found that its performance decreases as the number of network nodes increases. To cope with this problem, we have proposed to implement a TDMA scheme and we have seen that it sensibly improves the network performance.

Acknowledgments

The work of this paper has been partially supported by the Friuli Venezia Giulia region under the POR/FESR 2007–2013 programme, project LAK—Living for All Kitchen.

References

- [1] European Commission, *Energy 2020—A Strategy for Competitive, Sustainable and Secure Energy*, 2010.
- [2] L. Lampe, A. Tonello, and D. Shaver, “Power line communications for automation networks and smart grid,” *IEEE Communications Magazine*, vol. 49, no. 12, pp. 26–27, 2011.
- [3] A. Zaballos, A. Vallejo, and J. Selga, “Heterogeneous communication architecture for the smart grid,” *IEEE Network*, vol. 25, no. 5, pp. 30–37, 2011.
- [4] H. C. Ferreira, L. Lampe, J. Newbury, and T. G. Swart, *Power Line Communications: Theory and Applications for Narrowband and Broadband Communications Over Power Lines*, Wiley & Sons, New York, NY, USA, 2010.
- [5] V. C. Gungor, D. Sahin, T. Kocak et al., “Smart grid technologies: communication technologies and standards,” *IEEE Transactions on Industrial Informatics*, vol. 7, no. 4, pp. 529–539, 2011.
- [6] M. M. Rahman, C. S. Hong, S. Lee, J. Lee, M. A. Razzaque, and J. H. Kim, “Medium access control for power line communications: an overview of the IEEE 1901 and ITU-T G.hn standards,” *IEEE Communications Magazine*, vol. 49, no. 6, pp. 183–191, 2011.
- [7] HomeGrid Forum, *G.hn—Compatibility with Existing Home Networking Technologies*, 2009.
- [8] V. Suraci, A. Cimmino, R. Colella, G. Oddi, and M. Castrucci, “Convergence in home gigabit networks: implementation of the inter-MAC layer as a pluggable kernel module,” in *Proceedings of the IEEE 21st International Symposium on Personal Indoor and Mobile Radio Communications (PIMRC '10)*, pp. 2569–2574, Istanbul, Turkey, September 2010.
- [9] V. Miori, L. Tarrini, M. Manca, and G. Tolomei, “An open standard solution for domotic interoperability,” *IEEE Transactions on Consumer Electronics*, vol. 52, no. 1, pp. 97–103, 2006.
- [10] S. Wolff, P. G. Larsen, K. Lausdahl, A. Ribeiro, and T. S. Toftegaard, “Facilitating home automation through wireless protocol interoperability,” in *Proceedings of the International Symposium on Wireless Personal. Multimedia Communications*, September 2009.
- [11] D. Elshani and P. Francq, “The anatomy of a universal domotics integrator for globally interconnected devices,” in *Proceedings of the International Conference on Pervasive Systems and Computing*, pp. 17–23, June 2006.
- [12] S. Tompros, N. Mouratidis, M. Draaijer, A. Foglar, and H. Hrasnica, “Enabling applicability of energy saving applications on the appliances of the home environment,” *IEEE Network*, vol. 23, no. 6, pp. 8–15, 2009.
- [13] *IEEE P1905. 1/D06, IEEE Draft Standard for A Convergent Digital Home Network for Heterogeneous Technologies*, IEEE, 2012.
- [14] IEEE Standards Association, *IEEE Std. 802. 11-2012—Part 11: Wireless LAN Medium Access Control (MAC) and Physical Layer (PHY) Specifications*, IEEE, 2012, .
- [15] L. Chang, *White Paper—Making of IEEE 802. 3 Compliant Equipment*, National Semiconductor, 2003.

- [16] Multimedia over Coax Alliance, *MoCA 1.1 Specification for Device RF Characteristics*, 2012.
- [17] ZigBee Alliance, *ZigBee and Wireless Radio Frequency Coexistence*, 2008.
- [18] HomePlug Powerline Alliance, *HomePlug AV White Paper*, 2005.
- [19] ZigBee Alliance and HomePlug Powerline Alliance liaison, *Smart Energy Profile Version 2.0 Technical Requirements*, 2012.
- [20] ERDF, *PLC G3 Physical Layer Specification*.
- [21] ERDF, *PLC G3 MAC Layer Specification*.
- [22] V. Oksman and J. Zhang, "G.HNEM: the new ITU-T standard on narrowband PLC technology," *IEEE Communications Magazine*, vol. 49, no. 12, pp. 36–44, 2011.
- [23] L. D. Bert, S. D'Alessandro, and A. M. Tonello, "An Interconnection approach and performance tests for in-home PLC networks," in *Proceedings of the IEEE International Symposium on Power Line Communications and Its Applications*, Beijing, China, March 2012.
- [24] *IEEE Std 802.15.4-2006, Part 15.4: Wireless Medium Access Control (MAC) and Physical Layer (PHY) Specifications for Low-Rate Wireless Personal Area Networks (WPANs)*, IEEE, 2006.
- [25] A. Varga, *OMNeT++ User Manual*, 2011.
- [26] *INET Framework For OMNeT++ Manual*, 2012.
- [27] *MAX2990 Integrated Power-Line Digital Transceiver Programming Manual*, Maxim Integrated Products, 2010.
- [28] G. Bianchi, "IEEE 802.11-saturation throughput analysis," *IEEE Communications Letters*, vol. 2, no. 12, pp. 318–320, 1998.
- [29] S. Boyd and L. Vandenberghe, *Convex Optimization*, Cambridge University Press, 2004.